



Network Medicine-Based Repurposing of Mesalazine for Atherosclerosis Treatment

Jianhui Jiang¹ · Ziling Zheng¹ · Chongbo Jiang² · Tingbiao Wu¹ · Wei Shi³ · Mengchen Liu¹ · Qing Fan³ · Guozhen Cui¹

Received: 22 January 2025 / Accepted: 23 May 2025

© The Author(s), under exclusive licence to Springer Science+Business Media, LLC, part of Springer Nature 2025

Abstract

Atherosclerosis remains a leading cause of cardiovascular disease and mortality worldwide, despite advancements in statin therapies. Here, we aimed to identify potential anti-atherosclerosis drugs by an integrated approach combining network medicine-based prediction with empirical validation. Among the top drugs predicted by the preferred algorithm, mesalazine—a drug traditionally used to treat inflammatory bowel disease, was selected for in vivo validation in ApoE^{-/-} mouse model of atherosclerosis. After an 8-week treatment period, mesalazine significantly inhibited atherosclerosis progression by reducing total cholesterol (TC), triglyceride (TG), and low-density lipoprotein cholesterol (LDL-C) levels, while increasing high-density lipoprotein cholesterol (HDL-C) levels. Additionally, it decreased the plaque area and hepatic steatosis. Gene expression analysis via RT-qPCR revealed that mesalazine downregulated key genes associated with atherosclerosis. These findings highlight the potential of mesalazine as a repurposed anti-atherosclerosis drug and offer novel insights into drug screening for atherosclerosis treatment.

Keywords Atherosclerosis · Drug screening · Network medicine · Mesalazine

Abbreviations

| | |
|---------------------|--------------------------------------|
| AS | Atherosclerosis |
| AUC | Area Under the Curve |
| ApoE ^{-/-} | Apolipoprotein E knockout |
| HE | Hematoxylin eosin |
| Masson | Masson's Trichrome |
| RT-qPCR | Real time-quantitative PCR (RT-qPCR) |
| TC | Total cholesterol |
| TG | Triglycerides |

| | |
|------------|--|
| LDL-C | Low-density lipoprotein cholesterol |
| HDL-C | High-density lipoprotein cholesterol |
| MS | Mesalazine |
| Svt | Simvastatin |
| PPARG | Peroxisome roliferator-Activated Receptor Gamma |
| PTGS1 | Prostaglandin-Endoperoxide Synthase 1 |
| PTGS2 | Prostaglandin-Endoperoxide Synthase 2 |
| ALOX5 | Arachidonate 5-Lipoxygenase |
| IKKBK | Inhibitor of Nuclear Factor Kappa-B Kinase Subunit Beta |
| <i>MPO</i> | Myeloperoxidase |
| CHUK | Inhibitor of nuclear factor kappa-B kinase subunit alpha |
| CVD | Cardiovascular diseases |
| ROC | Receiver Operating Characteristic |
| PPI | Protein-protein interaction |
| LCC | Largest connected component |
| TPR | True Positive Rate |
| FPR | False Positive Rate |
| PFA | Paraformaldehyde |
| PBS | Phosphate Buffered Saline |
| AI | Atherosclerosis index |
| NF-κB | Nuclear Factor kappa B |

Associate Editor Nicola Smart oversaw the review of this article.

Jianhui Jiang and Ziling Zheng have contributed equally to this work.

✉ Qing Fan
fanqo@foxmail.com

✉ Guozhen Cui
cgzum@hotmail.com

¹ School of Bioengineering, Zhuhai Campus of Zunyi Medical University, Zhuhai 519000, China

² Beijing Road Outpatient Department, Northern Medical Branch of PLA General Hospital, Beijing 100094, China

³ Basic Medical Science Department, Zhuhai Campus of Zunyi Medical University, Zhuhai 519000, China

| | |
|---------------------|---|
| Ldlr ^{-/-} | Low-Density Lipoprotein Receptor knockout |
| LOX | Lysyl Oxidase |
| HFD | High-fat diet |

Introduction

Atherosclerosis, a chronic and progressive disease, is characterized by the accumulation of lipids, cholesterol, and inflammatory cells within arterial walls, leading to plaque formation and vascular occlusion. This pathological process substantially elevates the risk of cardiovascular disease (CVD) such as myocardial infarction and stroke, which are leading causes of global morbidity and mortality. In 2019, the number of prevalent cases of total CVD nearly reached 523 million, resulting in approximately 18.6 million deaths worldwide [1]. Currently, statins remain the cornerstone of atherosclerosis therapy, effectively reducing cholesterol and low-density lipoprotein (LDL) levels, thereby slowing disease progression [2]. However, their use, particularly among older individuals with multiple comorbidities, can induce neuromuscular side effects, including myalgia, myopathy, and cramps [3]. Statins have even been reported to potentially aggravate insulin resistance [4]. All these facts underscore the urgent need for the development of safer and more efficacious therapeutics for atherosclerosis.

Network medicine, an emerging interdisciplinary field, applies network science to elucidate the complex interrelationships within biological systems and disease mechanisms [5]. In drug discovery, it enhances the efficiency of drug research and development by clarifying the molecular interaction networks between diseases and drugs. This approach facilitates the identification of new indications for approved drugs, thereby accelerating the drug discovery process [6, 7]. Central of network medicine is the concept of disease modules, which are clusters of interconnected genes or proteins that collectively contribute to a disease phenotype. By identifying these modules, researchers can pinpoint critical nodes that may be targeted by approved drugs [8]. Network-based proximity measures assess the relationship between drug targets and disease-associated genes within the human interactome, promoting the identification of repurposable drugs [9]. Traditional drug discovery typically focuses on a single molecular target, often overlooking the broader functions of the biological network. In contrast, network medicine analyzes complex networks of molecular interactions, offering novel insights into disease pathogenesis and therapeutic strategies [10]. This holistic approach is particularly valuable for understanding complex diseases such as atherosclerosis,

shifting the focus from individual molecular targets to the broader network context [11, 12].

In this study, we applied the network medicine approach, complemented by literature mining, to identify potential anti-atherosclerosis drug candidates, as outlined in the study flowchart (Fig. 1). Notably, our predictive analysis indicated that mesalazine, a drug traditionally used to treat inflammatory bowel disease, could be repurposed for atherosclerosis treatment. This predictive result was validated by our experimental results, which demonstrated that mesalazine significantly modulated lipid profiles and reduced atherosclerotic plaque formation. Our molecular analysis revealed that the mechanisms underlying the effects of mesalazine involve genes such as prostaglandin-endoperoxide synthase 1 (PTGS1), prostaglandin-endoperoxide synthase 2 (PTGS2), peroxisome proliferator-activated receptor gamma (PPARG), arachidonate 5-lipoxygenase (ALOX5), inhibitor of nuclear factor kappa-B kinase subunit beta (IKBKB), and myeloperoxidase (MPO). These findings position mesalazine as a promising therapeutic candidate for atherosclerosis, highlighting the potential of network medicine to identify novel treatments for cardiovascular diseases.

Materials and Methods

Collection of Atherosclerosis Genes, Drugs and Drug Targets

To construct a comprehensive dataset, we integrated gene data causally related to atherosclerosis from 4 databases: Therapeutic Target Database (TTD) [13], Comparative Toxicogenomics Database (CTD) [14], UniProt [15], and DisGeNET [16]. To ensure high data quality, we performed an extensive literature review using PubMed employing keywords related to atherosclerosis, gene knockout, or gene overexpression to extract genes that are experimentally linked to atherosclerosis. Only genes with documented effects on disease phenotypes following genetic intervention were included in our dataset. This dual approach of database integration and literature verification provided a comprehensive and reliable gene list for atherosclerosis research. The Entrez gene ID for each gene was retrieved from the National Center for Biotechnology Information (NCBI) and archived in CSV format for subsequent data analysis. Mesalazine-target information was acquired from the Drug-Bank database [17].

Network Proximity Calculations

Network proximity calculations were performed in a protein-protein interaction (PPI) network consisting of 18,375

proteins (nodes) and 485,412 interactions (edges) as previously described [18]. The network proximity between atherosclerosis and all drugs in the DrugBank database was calculated using three different methods as previously described [9, 12]. All three methods employed the same dataset of drug targets. For the disease genes, two methods utilized the complete set of disease-related genes in Eq. 1 and Eq. 2, respectively. When comparing predictive ability using the area under the curve (AUC), results from Eq. 1 outperformed those from Eq. 2. To assess whether the selection of disease-related genes could influence the proximity results, the largest connected component (LCC) of the disease-related genes in the PPI network was extracted and applied in Eq. 1 as the third method.

$$d_c(S, T) = \frac{1}{\|T\|} \sum_{t \in T} \min_{s \in S} d(s, t) \quad (1)$$

$$d_c(S, T) = \frac{1}{\|S\| + \|T\|} \left[\sum_{s \in S} \min_{t \in T} d(s, t) + \sum_{t \in T} \min_{s \in S} d(s, t) \right] \quad (2)$$

$$Z\text{-score} = \frac{d_c(S, T) - \mu_{d_c}(S, T)}{\sigma_{d_c}(S, T)} \quad (3)$$

In Eqs. (1) and (2), S represents the set of disease-related genes, T represents the set of drug targets, $d(s, t)$ is the distance between gene s and target t in the PPI network, and $d_c(S, T)$ is the closest proximity between gene set S and target set T . To assess the statistical significance of the network distance between drugs and atherosclerosis, we formulated a reference distance distribution [9]. This distribution mirrors the expected distance between any two randomly chosen node sets in the PPI network, conserving the number of nodes and the degree of each node. Using this reference distance distribution, we calculated the relative significance of the proximity between drug and disease as in Eq. (3), where Z -score represents the relative significance, $\mu_{d_c}(S, T)$ is the mean of the reference distribution, and $\sigma_{d_c}(S, T)$ is the standard deviation of the reference distribution. A smaller Z -score signifies closer network proximity, and a Z -score < 0 with $P < 0.05$ was considered statistically significant [19]. Subsequently, the corresponding genes (targets) in the PPI were extracted and imported into Gephi 0.9.2 software for network visualization analysis as previously described [20].

Area under the Curve Analysis

The ROC (Receiver Operating Characteristic) curve is a commonly accepted performance measure for evaluating ranking quality [9]. We employed the Area Under the Curve (AUC) as a metric to assess the predictive ability

of the different methods used in calculating the proximity $d_c(S, T)$ and the relative significance Z -score. Specifically, we evaluated performance using all the disease genes as inputs for Eqs. (1) and (2), and by extracting the LCC of the disease genes and using it as input for Eq. (1). Positive drugs were obtained from FDA-approved indications data, representing “known drug-disease associations,” while “unknown drug-disease associations” served as negative controls. True Positive Rate (TPR) and False Positive Rate (FPR) were calculated at various thresholds for the associations of the two types of samples and plotted to generate ROC curves [21]. These ROC curves were used to assess the ability of the methods to predict drugs with therapeutic effects, with AUC values typically ranging from 0.5 to 1. An AUC greater than 0.5 indicates better performance, with values closer to 1 representing superior predictive accuracy.

Drug Ranking and Literature Analysis

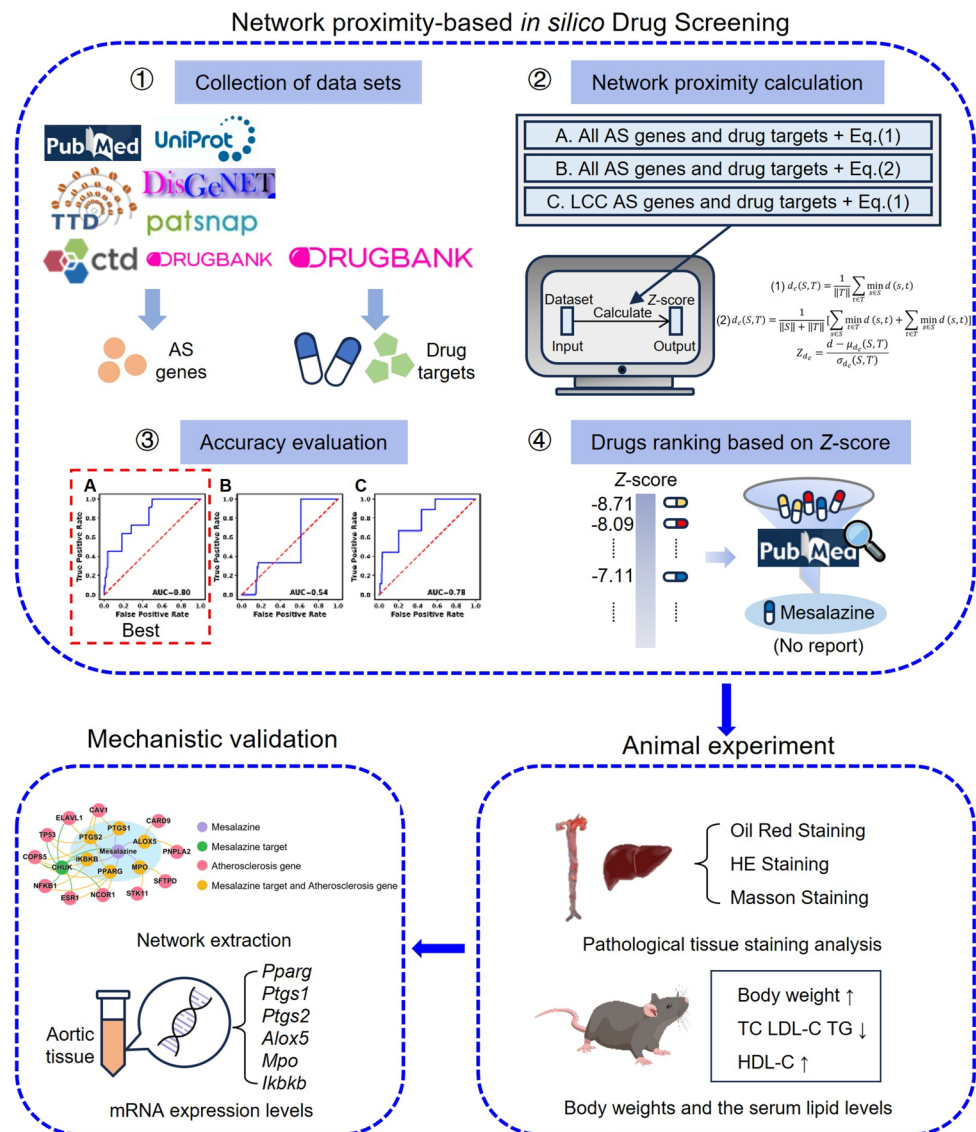
The network-predicted repurposable drugs were ranked in ascending order according to their Z -score values. The top 10 drugs were then meticulously reviewed through comprehensive literature analysis to identify any existing research reports linking these predicted drugs to atherosclerosis.

Animal Study

ApoE^{-/-} mice and C57BL/6 J mice, aged 8–10 weeks and weighing between 22–25 g, were obtained from Guangdong Medical Animal Experimental Center (Guangdong, China). Both male and female mice were included. The animals were maintained under controlled conditions as previously described [22]. They were provided ad libitum access to standard laboratory chow and water throughout the study. The experimental protocol was conducted in accordance with the Guide for the Use of Laboratory Animals.

After a one-week acclimatization period, 32 ApoE^{-/-} mice were randomly divided into four groups ($n = 8$ per group) with an equal 1:1 male-to-female ratio, as recommended by the literature [23]. The groups were as follows: vehicle group, receiving a solvent treatment; positive control group, treated with 5.3 mg/kg simvastatin; the low-dose mesalazine group, administered 20 mg/kg mesalazine; high-dose mesalazine group, given 60 mg/kg mesalazine. The dose of mesalazine was determined based on a previous report [24]. Additionally, a control group of C57BL/6 J mice ($n = 8$, with an equal 1:1 male-to-female ratio) was maintained on a standard diet. All experimental groups, except for the control group, were fed a high-fat diet for the study duration. After a 2-week dietary acclimation phase, the

Fig. 1 Schematic representation of the experimental workflow



ApoE^{-/-} mice were subjected to daily oral gavage, and their body weights were recorded weekly over an 8-week period.

Collection of Mouse Samples

After a 10-week feeding period, blood samples were collected from the mice, followed by anesthesia for dissection as previously described [25]. The aortas were carefully dissected from the aortic root to the branch of the common iliac artery. For each group, four aortas (with equal numbers of males and females) were immersed in PBS for Oil Red O staining. Another four vessels were sampled with equal tissue quantities from the aortic arch and fixed in 4% paraformaldehyde (PFA) for histopathological assessment of plaque formation, while the remaining segments were homogenized for real time-quantitative PCR (RT-qPCR) analysis. Additionally,

liver tissues were collected, with liver lobes separated and fixed in 4% PFA in preparation for pathological examination.

Pathological Morphology Analysis, Lipid Measurements and Atherogenic Index Calculations

Atherosclerotic plaques in the aorta were quantified using Oil Red O staining, hematoxylin and eosin (HE) staining, and Masson staining. Liver tissue was subjected to HE staining to assess hepatocellular steatosis, employing semi-quantitative grading scores as previously described [18]. Following the staining procedures, the aortic specimens and liver tissues were examined and photographed under a microscope. Subsequent analysis was conducted using Image-Pro Plus 6.0 software, with the images being analyzed by a blinded observer. Serum samples were analyzed

for total cholesterol (TC), triglycerides (TG), low-density lipoprotein cholesterol (LDL-C), and high-density lipoprotein cholesterol (HDL-C) using corresponding assessment kits. The atherogenic index was then calculated using the formula: atherogenic index = $[\text{TC (mmol/L)} - \text{HDL-C (mmol/L)}] / \text{HDL-C (mmol/L)}$.

Network Diagram Construction

The subnetwork of mesalazine targets and their directly connected atherosclerosis genes in the PPI network was extracted and imported into Gephi 0.9.2 software for visualization. This approach enabled an in-depth exploration of the underlying mechanisms governing drug action.

RT-qPCR Analysis

Total RNA was extracted from the carotid artery using Trizol reagent (Beyond, Shanghai, China). The RNA was then reverse transcribed into cDNA using HiScript II Q RT SuperMix (Vazyme, Shanghai, China). RT-qPCR was performed using a StepOne Plus Real-Time PCR System as previously described [26]. Relative gene expression levels were determined using the comparative Ct method. The primer sequences are listed in Table 1.

Statistical Analysis

Statistical analyses were performed using Graph-Pad Prism 8.0 software. Data are expressed as means \pm standard deviations ($\bar{x} \pm s$). For comparisons involving multiple groups, one-way analysis of variance (ANOVA) followed by Tukey's post hoc test was utilized for multiple comparisons. Statistical significance was defined as $P < 0.05$.

Results

Accuracy Comparison of Predicting Positive Drugs by the Three Methods

A comprehensive collection of 538 atherosclerosis-related genes was assembled through database queries and extensive literature reviews (Supplementary Table 1). From DrugBank database, 6,696 drug entries with defined targets were retrieved (Supplementary Table 2). Filtering criteria were set at $P < 0.05$ and $Z\text{-score} < 0$ for the results of three calculation methods. The filtered results were analyzed in ascending order of $Z\text{-score}$ values, yielding 11 identified drugs that have been approved for the treatment of atherosclerosis. The network proximity calculation

method using Eq. (1) with all disease genes demonstrated the highest performance achieving an AUC score of 0.80 (Fig. 2A). In contrast, the AUC scores for the other two methods were 0.54 and 0.78, respectively (Fig. 2B and C).

Drug Screening Results Based on Network Proximity

The $Z\text{-scores}$ from the optimal method were collected, with $Z\text{-score} < 0$ and $P < 0.05$ indicating statistical significance. The predicted drugs were prioritized in descending order based on the $Z\text{-score}$ values obtained through network analysis (Supplementary Table 3). The top 10 drugs, listed in Table 2, were selected for further scrutiny via literature review. Notably, a thorough literature search revealed no existing reports or studies elucidating the relationship between mesalazine and atherosclerosis, prompting its selection as a novel candidate drug for further experimental investigation.

Mesalazine Inhibits the Progression of Atherosclerosis in Mouse Aorta

The experimental design is depicted in Fig. 3A. Oil Red O staining of the mouse aorta revealed no noticeable red-colored areas in the control group, indicating the absence of atherosclerotic plaques. In contrast, the vehicle group exhibited substantial increase in red coloration, indicating plaque formation. Mesalazine-treated groups showed a marked reduction in red staining compared to the vehicle group (Fig. 3B). Quantitative analysis showed that the area of atherosclerotic plaques in the model group was significantly higher than that in the control group ($P < 0.0001$), and the percentage of atherosclerotic plaques in the low-dose mesalazine treatment group ($P = 0.0002$) and the high-dose treatment group ($P = 0.0041$) was significantly lower than that in the vehicle group (Fig. 3C).

Mesalazine Inhibits the Formation of Atherosclerotic Plaque in Mouse Aorta

HE staining of the aortic arch revealed an absence of visible plaques in the control group, whereas the vehicle group exhibited substantial atherosclerotic plaque formation. Mesalazine treatment significantly reduced the extent of atherosclerotic plaques compared to the vehicle group (Fig. 3D). The vehicle group showed extensive blue collagen staining within the plaques, which was absent in the control group. Notably, mesalazine treatment markedly decreased blue collagen staining in the arterial walls (Fig. 3E). Quantitative analysis revealed a significant decrease in plaque area following mesalazine treatment (Fig. 3F, $P < 0.05$). Masson staining further demonstrated

a significantly smaller area of blue collagen in the mesalazine-treated groups compared to the vehicle group, which exhibited a notably larger collagen-stained area than the control group (Fig. 3G, $P < 0.05$).

Mesalazine Mitigates Hepatic Steatosis in Mice

HE staining of liver tissue demonstrated that the control group maintained normal liver architecture with orderly hepatocytes and no noticeable swelling or fat vacuoles. In contrast, the vehicle group displayed significant structural disruption, characterized by widespread fat vacuolation. Both the positive control and mesalazine-treated groups displayed a substantial reduction in fat vacuolation compared to the vehicle group (Fig. 4A). Quantitative analysis of steatosis scores indicated a statistically significant decrease in hepatic steatosis in the mesalazine-treated groups, with a concentration-dependent effect observed compared to the vehicle group (Fig. 4B, $P < 0.05$).

Effects of Mesalazine on Lipid Levels and Atherogenic Index in Mice

After 10 weeks on a high-fat diet, mice in the vehicle group exhibited significantly higher body weights compared to the control group. Although the mice in the mesalazine-treated groups had lower body weights than those in the vehicle group, the difference was not statistically significant (Fig. 5A, $P > 0.05$). Serum levels of TC, TG, and LDL-C were significantly elevated in the vehicle group ($P < 0.05$), while HDL-C levels were significantly reduced ($P < 0.05$) compared to the control group. In the high-dose mesalazine group, there was a statistically significant reduction in TC, LDL-C, and TG levels compared to the vehicle group (Fig. 5B-D, $P < 0.05$). Additionally, HDL-C levels were significantly higher in the mesalazine-treated groups compared to the vehicle group (Fig. 5E, $P < 0.05$). The atherogenic index also showed a significant decrease in the mesalazine-treated groups compared to the vehicle group (Fig. 5F, $P < 0.05$).

Analysis of the Potential Regulatory Network of Mesalazine's Anti-Atherosclerotic Effects and Detection of mRNA Expression Levels of Related Genes

Network visualization analysis comprising 57 nodes and 82 edges, revealed that PTGS1, PTGS2, ALOX5, IKBKB, PPARG, and MPO were both drug targets and disease-associated genes, with CHUK identified solely as a drug target (Fig. 6A). The results of mRNA expression levels revealed that PTGS1, PTGS2, ALOX5, and IKBKB were downregulated in mesalazine-treated groups compared to the vehicle group. Notably, the high-dose mesalazine group exhibited a statistically significant reduction (Fig. 6B-E, $P < 0.05$). Furthermore, PPARG expression significantly increased (Fig. 6F, $P < 0.05$), while MPO expression decreased, although this change was not statistically significant (Fig. 6G, $P > 0.05$).

Discussion

In this study, we identified a novel potential use of mesalazine, a drug primarily used in the treatment of inflammatory bowel disease, as a treatment for atherosclerosis. Using network-based approach, we mapped drug targets and atherosclerosis-related genes onto a human PPI network. By calculating network proximity, we quantified the interactions between drugs and the disease, facilitating the identification of potential therapeutic candidates. After a comprehensive literature review, mesalazine was identified as a promising candidate for its potential anti-atherosclerotic effects. Subsequent animal experiments confirmed its efficacy of mesalazine in inhibiting the development of atherosclerosis. Histological analyses, including Oil Red O, HE, and Masson staining, revealed a significant reduction in atherosclerotic plaque formation and hepatic steatosis in mesalazine-treated mice. Additionally, mesalazine treatment resulted in decreased serum levels of TG, TC, and LDL-C, while increasing HDL-C levels.

Atherosclerosis, a chronic inflammatory disease, is characterized by the accumulation of lipids and inflammatory cells within arterial walls, leading to plaque formation.

Table 1 Sequences of primers used for qRT-PCR

| Gene ID | Gene symbol | Forward Primer | Reverse Primer |
|---------|--------------|----------------------------|---------------------------|
| 16,150 | <i>Ikbkb</i> | CAGAATCACAGCGGGCAGGAAG | GAGAGCAGATACAGGACAGGAGAG |
| 19,224 | <i>Ptgs1</i> | GCCAGAAGATAGCAGGTGTTGACTC | GTAGCCATCCGCAGTGACATTAGAG |
| 19,225 | <i>Ptgs2</i> | CTGGTGCCCTGGTCTGATGATGTATG | GGATGCTCCTGCTTGAGTATGTCTG |
| 17,523 | <i>Mpo</i> | CGAGTTCAAGTCATCACCCCTGTAGC | TGGAGAGTTGGAGGAGGCAATAGG |
| 11,689 | <i>Alox5</i> | GGTCGCTGCTGCCATGAGAAG | CAGTCGTCAGGAGGTGGTAGGAG |
| 19,016 | <i>Pparg</i> | AGGAGCCAGAACCCACAGAGAAG | TCAACCACAGCACAGGACATTAC |

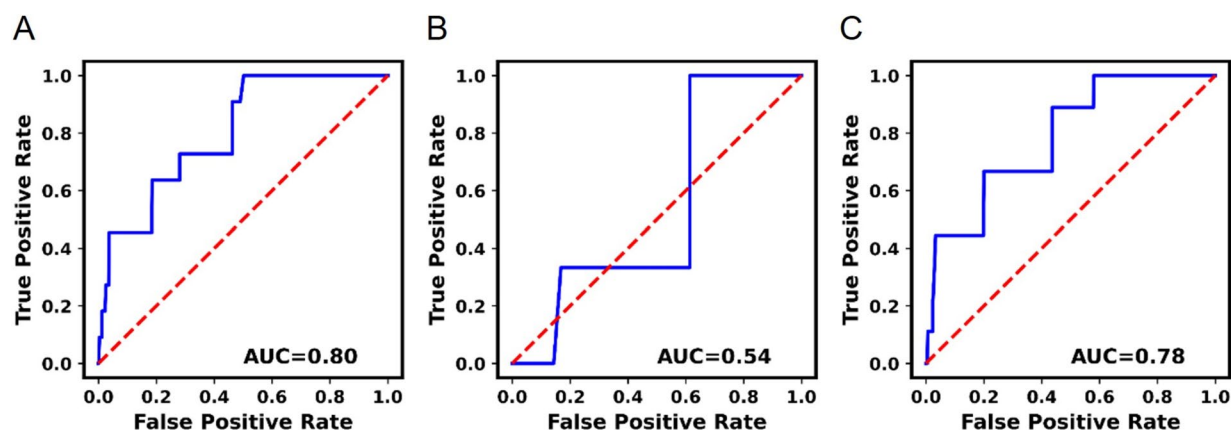


Fig. 2 The accuracy of predicting positive drugs using three different calculation methods. **A** ROC curve for network proximity calculation using Eq. (1). **B** ROC curve for network proximity calculation using

Eq. (2). **C** ROC curve for network proximity calculation using the LCC and Eq. (1)

Inflammation plays a key role throughout the disease progression, making anti-inflammatory strategies promising for treatment [38]. Clinical studies suggest that regulating inflammation can mitigate the complications associated with atherosclerosis, supporting the idea that anti-inflammatory therapy could be effective for treating atherosclerotic cardiovascular and cerebrovascular diseases [39]. Mesalazine, a well-established treatment for ulcerative colitis, inhibits the synthesis of prostaglandins and leukotrienes, key mediators of inflammation [40]. Its ability to reduce intestinal inflammation suggests it may have therapeutic potential for atherosclerosis through its anti-inflammatory effects. It is worth noting that the positive drug statin seems to display different actions in the ApoE^{-/-} mouse model of atherosclerosis. Sparrow et al. reported that simvastatin did not significantly alter lesion morphology in their mouse model, although it exhibited anti-inflammatory effects [54]. In contrast, our study observed a reduction in plaque area with statin treatment. We believe the difference may stem from the stage of atherosclerosis at the initiation of treatment. In their study,

statins were administered to ApoE^{-/-} mice at 16–20 weeks of age, when lesions may have already been more advanced. In our study, treatment began earlier, at 8–10 weeks of age, which could explain the more pronounced effect on plaque formation.

To further explore the mechanism underlying mesalazine's action against atherosclerosis, we mapped its drug targets within the PPI network and identified disease-associated genes that directly interact with these targets. Subsequently, potential regulatory network was constructed for its therapeutic effects, mRNA expression analysis revealed that mesalazine treatment upregulated PPARG and the downregulated PTGS1, PTGS2, ALOX5, and IKBKB. PPARs, including PPARG and PPARG, are molecular sensors of fatty acids and their derivatives, and are effective targets for treating lipid metabolic syndromes such as obesity, atherosclerosis, and dyslipidemia [41, 42]. Our findings suggest that mesalazine possesses both anti-atherosclerotic and lipid-lowering effects. PPARG, a transcription factor involved in lipid metabolism, exhibits strong tissue-protective and anti-inflammatory

Table 2 Top 10 drugs ranked by network proximity

| Rank | DrugBank ID | Drug name | Z – score | Related to AS or not | Reference |
|------|----------------|----------------------|--------------|----------------------|-----------|
| 1 | DB06521 | Ertiprotafib | –8.71 | Yes | [27, 28] |
| 2 | DB02709 | Resveratrol | –8.09 | Yes | [29] |
| 3 | DB01017 | Minocycline | –8.06 | Yes | [30, 31] |
| 4 | DB00945 | Acetylsalicylic acid | –7.57 | Yes | [32] |
| 5 | DB05187 | Elafibranor | –7.49 | Yes | [33] |
| 6 | DB09006 | Clinofibrate | –7.49 | Yes | [34] |
| 7 | DB00244 | Mesalazine | –7.11 | NO | - |
| 8 | DB09568 | Omega-3 fatty acids | –6.92 | Yes | [35] |
| 9 | DB01393 | Bezafibrate | –6.79 | Yes | [36] |
| 10 | DB13873 | Fenofibric acid | –6.61 | Yes | [37] |

“–” indicates that no similar correlation has been reported in the literature

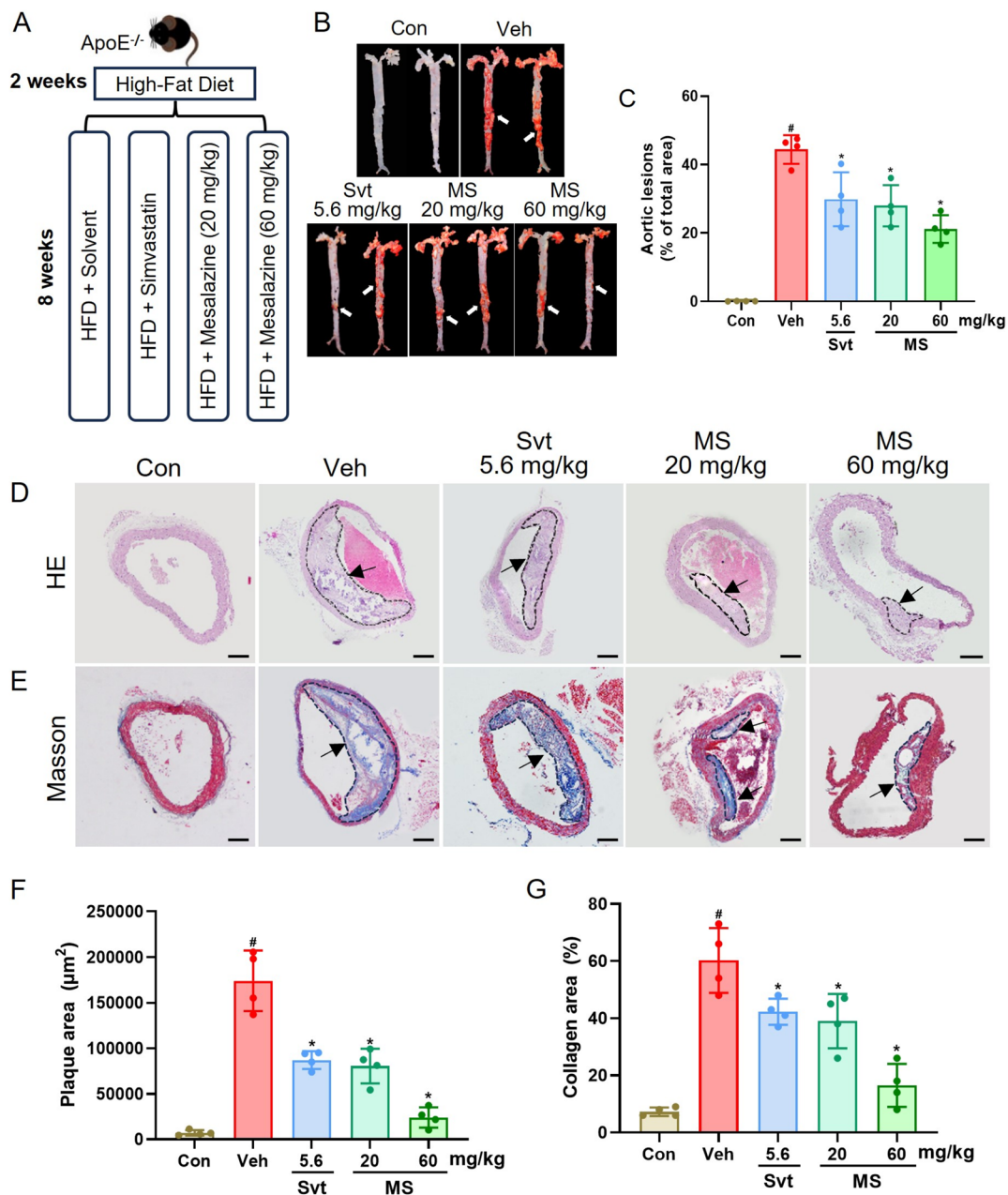


Fig. 3 Effects of mesalazine on atherosclerosis progression in mice. **A** The experimental design and drug administration method in ApoE^{-/-} mice treated daily with solvent, simvastatin, or mesalazine. **B** Aortic Oil Red O staining. White arrows indicate atherosclerotic plaques. **C** The percentage of plaque area relative to the total arterial area. **D** Aortic HE staining showing atherosclerotic plaques indicated

by black arrows. **E** Aortic Masson staining showing collagen fibers indicated by black arrows. **F** Quantitative analysis of the plaque area by aortic HE staining. **G** Collagen content was quantified by aortic Masson staining. Compared to the control group, #*P* < 0.05; compared to the vehicle group, **P* < 0.05. Scale bar: 100 μm. Svt: simvastatin, MS: mesalazine

properties, playing crucial role in mediating the anti-atherosclerotic effects associated with HDAC inhibition [43]. Additionally, PPARG activation suppresses the inflammatory response in macrophages [44]. Therefore, we hypothesize that mesalazine regulates lipid metabolism, promotes cholesterol removal from macrophages, and reduces foam cell formation by activating the PPAR pathway and increasing

PPARG expression, thereby ameliorating atherosclerosis in ApoE^{-/-} mice fed a high-fat diet.

Furthermore, our results showed that mesalazine inhibited the expression of PTGS1 and PTGS2 genes in ApoE^{-/-} mice. Prostaglandins play significant roles in vascular inflammation, smooth muscle cell proliferation, and the progression of atherosclerosis. PTGS1 and PTGS2, also known as

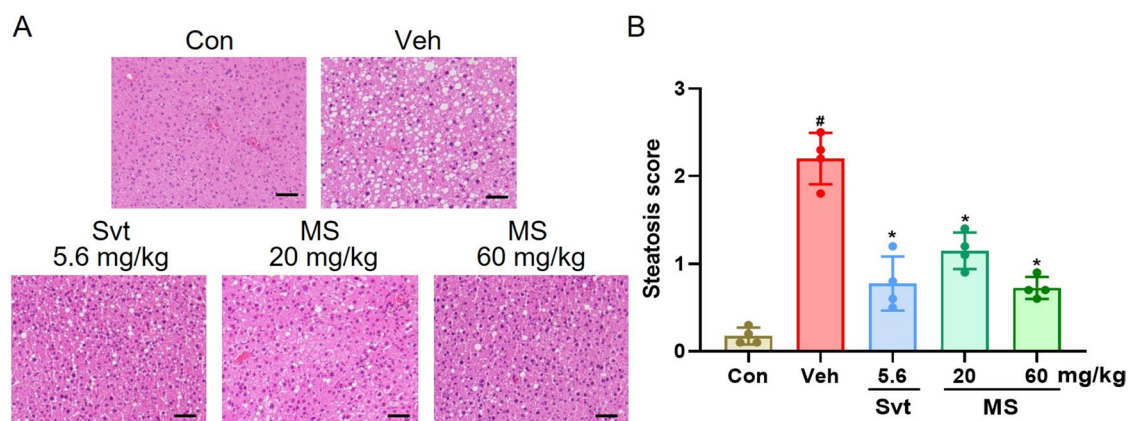
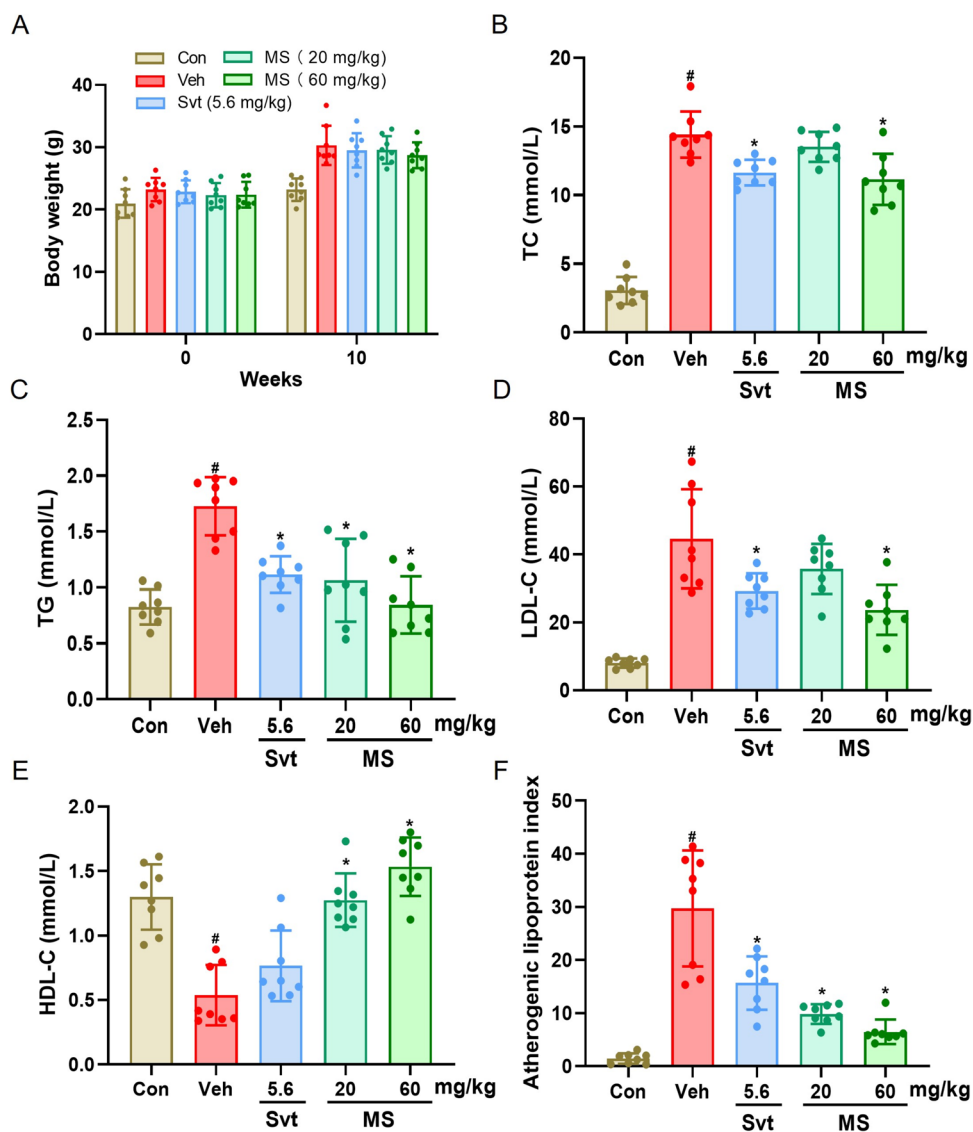


Fig. 4 Effects of mesalazine on fat accumulation and degeneration in mouse liver tissue. **A** HE staining of liver tissue. **B** Liver tissue steatosis assessment score. Compared to the control group, $^{\#}P < 0.05$;

compared to the vehicle group $^*P < 0.05$. Scale bar: 50 μ m. Svt, simvastatin; Ms, mesalazine

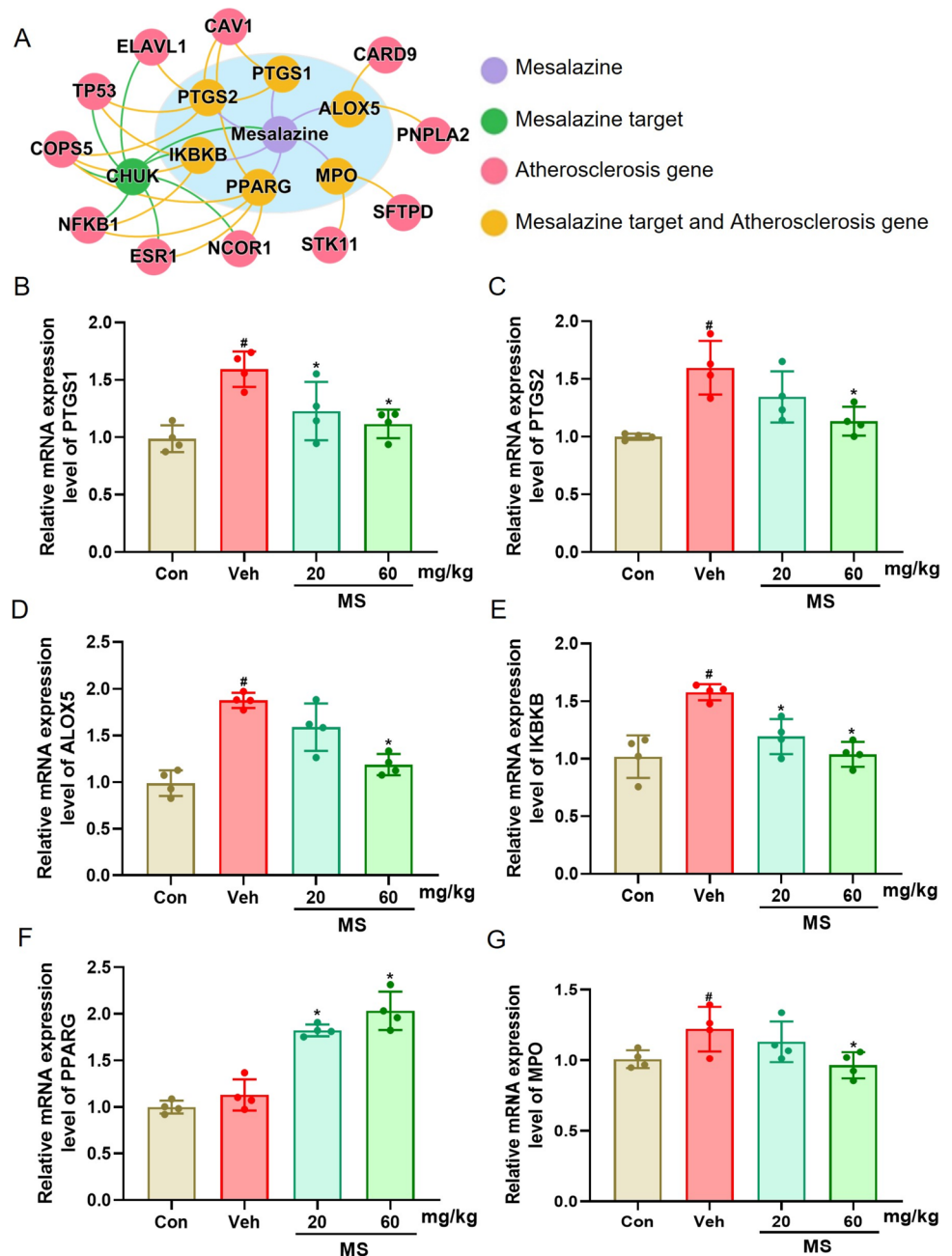
Fig. 5 Effects of mesalazine on body weight, serum lipids and atherogenic index in mice. **A** Body weight, **(B)** serum TC, **(C)** serum TG, **(D)** serum LDL-C, **(E)** serum HDL-C, and **(F)** atherogenic index. Compared to the control group, $^{\#}P < 0.05$; compared to the vehicle group, $^*P < 0.05$. Svt: simvastatin, MS: mesalazine



prostaglandin-endoperoxide synthase 1 and 2, convert arachidonic acid into the prostaglandin precursor PGH2 [45]. Non-steroidal anti-inflammatory drugs reduce prostaglandin synthesis, and exerting anti-inflammatory and analgesic effects. Knockout of PTGS1 has been shown to reduce atherosclerotic plaque formation in ApoE^{-/-} mice [46]. Additionally, simultaneous inhibition of PTGS2 and ALOX5 significantly reduces neointimal hyperplasia induced by vascular inflammation and injury [47]. Based on these findings, we speculate that mesalazine may interfere with the development of atherosclerotic lesions by inhibiting PTGS expression and prostaglandin synthesis.

Myeloperoxidase (MPO), a leukocyte-derived enzyme, reduces the levels of the anti-inflammatory molecule nitric oxide and produces oxidant precursors such as hypochlorous acid and nitrogen dioxide [48]. MPO plays a crucial role in the pro-inflammatory response and cell activation, regulating various inflammatory processes and promoting the development of atherosclerosis [49]. The NF- κ B signaling pathway, regulated by the transcription factor NF- κ B, is a key inflammatory signaling pathway. IKBKB, the main catalytic subunit of the IKK complex, is essential for the classical activation of the NF- κ B pathway by inflammatory mediators [50]. Knockout of IKBKB in vascular smooth muscle cells has been shown

Fig. 6 Network visualization of the relationship between mesalazine targets and atherosclerosis-associated genes and detection of mRNA expression levels of related genes. **A** Network diagram showing the relationship between mesalazine targets and atherosclerosis-associated genes. RT-qPCR analysis of relative mRNA expression levels in aortic arch. The genes evaluated included (**B**) PTGS1, (**C**) PTGS2, (**D**) ALOX5, (**E**) IKBKB, (**F**) PPARG, and (**G**) MPO. The nodes are colored as follows: purple, mesalazine (drug); yellow, overlapping target gene between the drug and disease; pink, genes directly connecting the disease and the drug; and green, unique target of mesalazine. Compared to the control group, # $P < 0.05$; compared to the vehicle group, * $P < 0.05$. MS: mesalazine



to reduce vascular inflammation and atherosclerosis progression [50]. Leukotrienes, abundant in atherosclerotic plaques, promote monocyte adhesion to endothelial cells, facilitate the transformation of monocyte to macrophages and foam cells, and enhance the proliferation and migration of vascular smooth muscle cells [51]. ALOX5, a rate-limiting enzyme in leukotriene biosynthesis, is highly expressed in the atherosclerotic plaques of ApoE^{-/-} and Ldlr^{-/-} mice. ALOX5 knockout has been shown to significantly reduce plaque formation [52, 53]. Therefore, it is logical to speculate that mesalazine may reduce the inflammatory response by decreasing the gene expression levels of inflammatory mediators such as MPO, IKBKB, and ALOX5, thereby inhibiting the development of atherosclerosis. Mesalazine's effects may involve modulation of the NF-κB and LOX signaling pathways, in addition to regulating lipid metabolism.

Despite these promising findings, several limitations should be acknowledged. First, we observed gene expression changes (e.g., PTGS1, PPARG, ALOX5), but did not conduct functional assays or protein-level validation, such as Western blot analysis, to further validate the proposed mechanisms. Second, although ApoE^{-/-} mice are widely used in atherosclerosis research, they do not fully replicate human atherosclerosis, so clinical validation in human studies is needed. Third, while mesalazine is known for its anti-inflammatory effects, further research is needed to understand its mechanism of reducing plasma cholesterol level. Finally, we used both male and female mice in this study, recognizing that sex is an important biological variable. Future studies with larger sample sizes should explore potential sex-specific differences in disease progression.

Conclusions

By combining network proximity calculations and experimental validation, we identified mesalazine as a potential therapeutic agent with anti-atherosclerotic properties. Animal studies confirmed that mesalazine effectively regulates blood lipid levels and reduces the formation of atherosclerotic plaques in ApoE^{-/-} mice fed a high-fat diet. Furthermore, mesalazine modulated the expression of key genes involved in atherosclerosis, including PPARG, ALOX5, IKBKB, PTGS1, and PTGS2. These findings provide new insights into mesalazine's potential as an anti-atherosclerotic drug and demonstrate the use of network medicine in discovering novel treatments for cardiovascular diseases.

Supplementary Information The online version contains supplementary material available at <https://doi.org/10.1007/s12265-025-10637-8>.

Author Contribution Jianhui Jiang: Methodology, Investigation, Data curation, Formal analysis, Visualization, Writing-original draft. Ziling Zheng: Methodology, Writing-review & editing, Visualization.

Jiang Chongbo: Methodology, Formal analysis, Validation. Tingbiao Wu: Validation, Methodology, Formal analysis. Wei Shi: Supervision, Funding acquisition. Mengchen Liu: Investigation, Data curation, Formal analysis. Qing Fan: Project Administration, Resources, Writing-review & editing. Guozhen Cui: Methodology, Project Administration, Supervision, Resources, Funding acquisition.

Funding This work was funded by grants from the Guizhou Province Science and Technology Program (ZK[2022]General 587), National Natural Science Foundation of China (82160684) and Innovation Team Project by the Department of Education of Guangdong Province (Grant No.2024 KCXTD005).

Data Availability The datasets generated during and/or analyzed during the current study are available from the corresponding author on reasonable request.

Declarations

Human and Animal Rights All of the animal experiments were approved by the Animal Ethics and the Use Committee of Zunyi Medical University protocol (ethics approval number: ZMU21-2403-103). No human studies were performed by the authors for this article.

Competing interest The authors declare that they have no conflict of interest.

References

1. Roth GA, et al. Global Burden of Cardiovascular Diseases and Risk Factors, 1990–2019: Update From the GBD 2019 Study. *J Am Coll Cardiol*. 2020;76(25):2982–3021.
2. Jensen LO, et al. Regression of coronary atherosclerosis by simvastatin: a serial intravascular ultrasound study. *Circulation*. 2004;110(3):265–70.
3. Attardo S, et al. Statins Neuromuscular Adverse Effects. *Int J Mol Sci*. 2022;23(15):8364.
4. She J, et al. Statins aggravate insulin resistance through reduced blood glucagon-like peptide-1 levels in a microbiota-dependent manner. *Cell Metab*. 2024;36(2):408–21 e5.
5. Ma M, et al. Network Medicine: A Potential Approach for Virtual Drug Screening. *Pharmaceuticals (Basel)*. 2024;17(7).
6. Ayar ES, et al. Network Medicine: From Conceptual Frameworks to Applications and Future Trends. *IEEE Trans Mol Biol Multi-Scale Commun*. 2023;9(3):374–81.
7. Loscalzo J. Molecular interaction networks and drug development: Novel approach to drug target identification and drug repositioning. *FASEB J*. 2023;37(1): e22660.
8. Menche J, et al. Disease networks. Uncovering disease-disease relationships through the incomplete interactome. *Science*. 2015;347(6224):1257601.
9. Guney E, et al. Network-based in silico drug efficacy screening. *Nat Commun*. 2016;7:10331.
10. Ma M, et al. Network Medicine: A Potential Approach for Virtual Drug Screening. 2024;17(7):899.
11. Barabasi AL, et al. Network medicine: a network-based approach to human disease. *Nat Rev Genet*. 2011;12(1):56–68.
12. Fiscon G, et al. A Comparison of Network-Based Methods for Drug Repurposing along with an Application to Human Complex Diseases. *Int J Mol Sci*. 2022;23(7):3703.
13. Zhou Y, et al. TTD: Therapeutic Target Database describing target druggability information. *Nucleic Acids Res*. 2024;52(D1):D1465–77.

14. Davis AP, et al. Comparative Toxicogenomics Database (CTD): update 2023. *Nucleic Acids Res.* 2023;51(D1):D1257–62.
15. UniProt: the Universal Protein Knowledgebase in 2023. *Nucleic Acids Res.* 2023;51(D1):D523–D31.
16. Piñero J, et al. The DisGeNET knowledge platform for disease genomics: 2019 update. *Nucleic Acids Res.* 2020;48(D1):D845–55.
17. Knox C, et al. DrugBank 6.0: the DrugBank Knowledgebase for 2024. *Nucleic Acids Res.* 2024;52(D1):D1265–D75.
18. Wang Y, et al. Golden bile powder prevents drunkenness and alcohol-induced liver injury in mice via the gut microbiota and metabolic modulation. *Chin Med.* 2024;19(1):39.
19. Ren A, et al. Integrating animal experiments, mass spectrometry and network-based approach to reveal the sleep-improving effects of Ziziphi Spinosae Semen and γ -aminobutyric acid mixture. *Chin Med.* 2023;18(1):99.
20. Han H, et al. Mitochondrial complex I inhibition by homoharringtonine: A novel strategy for suppression of chronic myeloid leukemia. *Biochem Pharmacol.* 2023;218: 115875.
21. Huang J, et al. Using AUC and accuracy in evaluating learning algorithms. 2005;17:299–310.
22. Wu T, et al. Identification of VDAC1 as a cardioprotective target of Ginkgolide B. *Chem Biol Interact.* 2024;406: 111358.
23. Robinet P, et al. Consideration of Sex Differences in Design and Reporting of Experimental Arterial Pathology Studies-Statement From ATVB Council. *Arterioscler Thromb Vasc Biol.* 2018;38(2):292–303.
24. Rajesh KM, et al. Effect of chronic low-dose treatment with chitooligosaccharides on microbial dysbiosis and inflammation associated chronic ulcerative colitis in Balb/c mice. *Naunyn Schmiedeberg's Arch Pharmacol.* 2024;397(3):1611–22.
25. Huang T, et al. Camellia oil (*Camellia oleifera* Abel.) treatment improves high-fat diet-induced atherosclerosis in apolipoprotein E (ApoE)^{-/-} mice. *Microbiota Food Health.* 2023;42(1):56–64.
26. Shi W, et al. Identification of dihydrotanshinone I as an ERp57 inhibitor with anti-breast cancer properties via the UPR pathway. *Biochem Pharmacol.* 2021;190: 114637.
27. Shrestha S, et al. PTP1B inhibitor Ertiprotafib is also a potent inhibitor of IkappaB kinase beta (IKK-beta). *Bioorg Med Chem Lett.* 2007;17(10):2728–30.
28. Erbe DV, et al. Ertiprotafib improves glycemic control and lowers lipids via multiple mechanisms. *Mol Pharmacol.* 2005;67(1):69–77.
29. Raj P, et al. A Comprehensive Analysis of the Efficacy of Resveratrol in Atherosclerotic Cardiovascular Disease, Myocardial Infarction and Heart Failure. *Molecules.* 2021;26(21).
30. Shahzad K, et al. Minocycline reduces plaque size in diet induced atherosclerosis via p27(Kip1). *Atherosclerosis.* 2011;219(1):74–83.
31. Say PR, et al. Hyperpigmentation of an Atherosclerotic Carotid Artery Plaque in a Patient on Chronic Suppressive Minocycline Therapy. *Ann Vasc Surg.* 2021;75(533):e1–4.
32. Roth L, et al. Acetylsalicylic Acid Reduces Passive Aortic Wall Stiffness and Cardiovascular Remodelling in a Mouse Model of Advanced Atherosclerosis. *Int J Mol Sci.* 2021;23(1).
33. Tsai HC, et al. Elafibranor Inhibits Chronic Kidney Disease Progression in NASH Mice. *Biomed Res Int.* 2019;2019:6740616.
34. Kinoshita M, et al. Japan Atherosclerosis Society (JAS) Guidelines for Prevention of Atherosclerotic Cardiovascular Diseases 2017. *J Atheroscler Thromb.* 2018;25(9):846–984.
35. Calder PC. The role of marine omega-3 (n-3) fatty acids in inflammatory processes, atherosclerosis and plaque stability. *Mol Nutr Food Res.* 2012;56(7):1073–80.
36. de Faire U, et al. Retardation of coronary atherosclerosis: the Bezafibrate Coronary Atherosclerosis Intervention Trial (BECAIT) and other angiographic trials. *Cardiovasc Drugs Ther.* 1997;11(Suppl 1):257–63.
37. Voros S, et al. Cardiovascular computed tomographic assessment of the effect of combination lipoprotein therapy on coronary arterial plaque: rationale and design of the AFRICA (Atorvastatin plus Fenofibrate acid in the Reduction of Intermediate Coronary Atherosclerosis) study. *J Cardiovasc Comput Tomogr.* 2010;4(3):164–72.
38. Engelen SE, et al. Therapeutic strategies targeting inflammation and immunity in atherosclerosis: how to proceed? *Nat Rev Cardiol.* 2022;19(8):522–42.
39. Soehnlein O, Libby P. Targeting inflammation in atherosclerosis - from experimental insights to the clinic. *Nat Rev Drug Discov.* 2021;20(8):589–610.
40. Sandborn WJ, Hanauer SB. Systematic review: the pharmacokinetic profiles of oral mesalazine formulations and mesalazine pro-drugs used in the management of ulcerative colitis. *Aliment Pharmacol Ther.* 2003;17(1):29–42.
41. Evans RM, et al. PPARs and the complex journey to obesity. *Nat Med.* 2004;10(4):355–61.
42. Gross B, et al. PPARs in obesity-induced T2DM, dyslipidaemia and NAFLD. *Nat Rev Endocrinol.* 2017;13(1):36–49.
43. Gao Q, et al. Enhancing PPAR γ by HDAC inhibition reduces foam cell formation and atherosclerosis in ApoE deficient mice. *Pharmacol Res.* 2020;160: 105059.
44. Zhang L, Chawla A. Role of PPARgamma in macrophage biology and atherosclerosis. *Trends Endocrinol Metab.* 2004;15(10):500–5.
45. Cabrera RA, et al. Prostaglandin-endoperoxide synthase (PTGS1 and PTGS2) expression and prostaglandin production by normal monkey ovarian surface epithelium. *Fertil Steril.* 2006;86(4 Suppl):1088–96.
46. Gautier-Veyret E, et al. Intermittent hypoxia-activated cyclooxygenase pathway: role in atherosclerosis. *Eur Respir J.* 2013;42(2):404–13.
47. Kirkby NS, et al. COX-2 protects against atherosclerosis independently of local vascular prostacyclin: identification of COX-2 associated pathways implicate Rgl1 and lymphocyte networks. *PLoS ONE.* 2014;9(6): e98165.
48. McMillen TS, et al. Expression of human myeloperoxidase by macrophages promotes atherosclerosis in mice. *Circulation.* 2005;111(21):2798–804.
49. Cheng D, et al. Inhibition of MPO (Myeloperoxidase) Attenuates Endothelial Dysfunction in Mouse Models of Vascular Inflammation and Atherosclerosis. *Arterioscler Thromb Vasc Biol.* 2019;39(7):1448–57.
50. Sui Y, et al. IKK β links vascular inflammation to obesity and atherosclerosis. *J Exp Med.* 2014;211(5):869–86.
51. Koshy AN, et al. A prospective natural history study of coronary atherosclerosis following liver transplantation. *Atherosclerosis.* 2022;344:40–8.
52. Uz T, et al. Effects of MK-886, a 5-lipoxygenase activating protein (FLAP) inhibitor, and 5-lipoxygenase deficiency on the forced swimming behavior of mice. *Neurosci Lett.* 2008;436(2):269–72.
53. Kasikara C, et al. The role of non-resolving inflammation in atherosclerosis. *J Clin Invest.* 2018;128(7):2713–23.
54. Sparrow CP, et al. Simvastatin has anti-inflammatory and anti-atherosclerotic activities independent of plasma cholesterol lowering. *Arterioscler Thromb Vasc Biol.* 2001;21(1):115–21.

Publisher's Note Springer Nature remains neutral with regard to jurisdictional claims in published maps and institutional affiliations.

Springer Nature or its licensor (e.g. a society or other partner) holds exclusive rights to this article under a publishing agreement with the author(s) or other rightsholder(s); author self-archiving of the accepted manuscript version of this article is solely governed by the terms of such publishing agreement and applicable law.